MOISTURE CONTENT EFFECTS ON THE RHEOLOGY AND STRUCTURAL STABILITY OF REMOLDED PADDY SOIL: ROTATIONAL RHEOMETRY

/

重塑水田土壤含水率对流变特性与结构稳定性的影响-基于旋转流变测试

Tianyu YANG [1,2], Weiming YI [1,2], Zhengwei LI [3], Hao WANG [1,2]

[1] School of Agricultural Engineering and Food Science, Shandong University of Technology, Zibo 255000, China;
[2] Shandong Research Center of Engineering & Technology for Clean Energy, Zibo 255000, China;
[3] School of Mechanical Engineering, Shandong University of Technology, Zibo 255000, China.
Tel: 19811729383; E-mail: yty676766948@163.com
DOI: https://doi.org/10.35633/inmateh-78-76

Keywords: *paddy soil; rheological properties; moisture content; viscoelasticity; stability; trafficability*

ABSTRACT

The rheological behavior of paddy soil plays a critical role in determining traction resistance, trafficability, and the operational performance of agricultural machinery. This study quantified the effects of moisture content on the steady-state and dynamic rheological properties of remolded paddy soil using a rotational rheometer. Soil samples were prepared at four moisture contents (23%, 26%, 29%, and 32%) and tested under steady shear and oscillatory loading conditions. Steady shear tests (0.1-100 s^{-1}) revealed pronounced shear-thinning behavior, which was well described by a power-law model ($n < 1$). Within this shear rate range, the apparent viscosity decreased from 11.57-1600 Pa·s at 23% moisture content to 1.343-238.7 Pa·s at 32%. Amplitude sweep tests indicated a transition from solid-like to liquid-like behavior, with the yield strain increasing approximately linearly with moisture content, while the yield modulus decreased. The loss factor increased with strain following a power-law relationship, and the fitted exponent decreased from 0.449 to 0.336 as moisture content increased. Frequency sweep tests identified a crossover frequency of approximately 40 Hz, at which the dominant response shifted from viscous- to elastic-dominated behavior under the test conditions. These results provide quantitative parameters and critical thresholds for understanding the structural stability of paddy soil under cyclic loading, and offer guidance for the optimization of running gear design and anti-slip/anti-sinkage strategies in paddy-field machinery.

摘要

水田土壤的流变行为直接影响农业机械的耕作阻力、行走通过性及作业质量。为探究含水率对水田土壤流变力学特性的影响规律，本研究采用旋转流变仪，对不同含水率（23%、26%、29%、32）的重塑水田土壤进行了稳态流变和动态流变试验。结果表明：1）水田土壤表现出显著的剪切稀化特性，符合幂律模型（n<1），为典型假塑性流体。2）水田土壤存在临界屈服应变点，且临界屈服应变随含水率增加呈线性增加趋势，说明随含水率增加固-液转化过程越慢，损耗因子随剪切应变增加呈幂函数式上升，明确了土壤结构失稳的临界条件。3）随着频率逐渐升高，存在临界频率使得土壤的主导力学行为会发生从类流体到类固体转变。研究构建了以含水率为变量的水田土壤流变状态演化关系，定量和定性地表征了水田土壤的流变特性，可为水田作业机械行走机构优化设计提供理论依据和数据支撑，对机械防滑防陷研究具有指导性意义。

INTRODUCTION

As a typical air-water-particle three-phase complex system, the mechanical properties of paddy soil determine the operating efficiency, trafficability and energy consumption level of agricultural machinery in the field. In the process of tillage, sowing and harvesting, the walking mechanism is faced with problems such as subsidence, sliding, high adhesion and high traction resistance between the working parts and the soil, which are related to the mechanical properties of the soil. Moisture content is the most core and active environmental factor affecting soil mechanical properties. Therefore, revealing the intrinsic relationship between moisture content and paddy soil mechanical properties has important theoretical and practical significance for the development of efficient and low-consumption agricultural equipment.

Domestic and foreign scholars have carried out extensive research on the mechanical properties of soil. Traditional soil mechanics test methods, such as direct shear test, triaxial compression test and bearing test, have laid a solid foundation for understanding the strength, deformation and bearing capacity characteristics of soil.

However, most of these methods focus on the ultimate strength characteristics of soil at the moment of failure. In the actual operation process, the stress process of the soil is closer to a continuous dynamic process of deformation, flow and even destruction. For example, the wheel squeezes the soil to make its lateral flow behavior, which not only includes plastic failure, but also includes viscoelastic response and flow behavior. Traditional mechanical tests are difficult to fully predict the internal mechanical performance of soil in the process of dynamic operation. " Rheology " originated from the discussion of the ancient Greek philosopher Heractitusd, and its thought can be summarized as " all things flow " *(Tian., 2023)*. As a typical rheological material, paddy soil exhibits both solid-like elastoplastic behavior and liquid-like flow behavior.

Regarding rheological model research, scholars have established various empirical or semi-empirical models such as the Bekker pressure-sinkage model and the Reece model. Since the 1980s, researchers like *Pan et al, (1983)*, have systematically studied the rheological properties of paddy soils in southern China, proposing the use of the four-element Burgers model to describe their stress-strain-time relationships. Subsequently, *Luo (1990), Ji (2004)*, and others further investigated the rheological parameters of paddy soil and their influencing factors through laboratory tests *(Sun et al., 2022; Hu et al., 2024)*. In recent years, with advancements in testing technology, rotational rheometers have been gradually introduced into soil rheology research. Scholars have systematically studied the effects of moisture content, resting time, tillage methods, and other factors on the steady-state rheological properties of different soil types *(Zhang et al., 2023; Liang et al., 2023; Liang et al., 2024)*. However, existing research has mostly focused on steady-state tests of dryland soils, high-water-content sediments *(Adebiyi et al., 2021; Xu et al., 2017)*, or clays *(Khramchenkov., 2003; Ni et al., 2020; Rakshith et al., 2018)*. Studies on the dynamic rheological response of paddy soil, particularly those systematically revealing its rheological evolution mechanism by combining steady-state and dynamic tests, are still relatively scarce.

Addressing the above issues, this study takes typical remolded paddy soil as the subject. Using a rotational rheometer, steady-state and dynamic shear tests are conducted to systematically investigate the rheological mechanical properties of paddy soil under different moisture content conditions. The aim is to establish quantitative relationship models between moisture content and key rheological parameters, thereby revealing the rheological behavior patterns of paddy soil. The research findings are intended to provide theoretical and experimental support for the design of paddy machinery running gear and the development of resistance-reduction and sinkage-prevention technologies.

MATERIALS AND METHODS

Experimental materials

The paddy soil used in the experiment was collected from Zibo City, Shandong Province, China. The soil was air-dried, crushed, and sieved to remove impurities such as small stones in accordance with the Chinese standard for geotechnical testing methods (GB/T 50123-2019). The particle size classification of soils commonly follows two international standards: the International Soil Science Society (ISSS)*(Nachtergaele & Spaargaren)* system and the United States Department of Agriculture (USDA)*(USDA 1999)* system. The classification criteria for both systems are summarized in Table 1. This study adopts the ISSS system for soil classification.

Table 1

Standard classification systems for soil particle size distribution

Category	Sand/mm	Silt/mm	Clay/mm
ISSS	2~0.02	0.02~0.002	＜0.002
USDA	2~0.05	0.05~0.002	＜0.002

The sedimentation velocity of soil particles in solution conforms to Stokes' law. The time required for soil particles of different diameters to settle a certain distance in water varies with temperature. During this period, the density of the soil suspension at a specific depth is measured using a specialized hydrometer, allowing calculation of the content of soil particles smaller than a certain size *(Wei et al., 2017)*. The testing process is illustrated in Figure 1. The tested soil was identified as neutral; therefore, a sodium oxalate solution was selected as the dispersing agent for the experiment. The results indicated that the average sand content was 43.10%, the average silt content was 33.97%, and the average clay content was 22.93%.

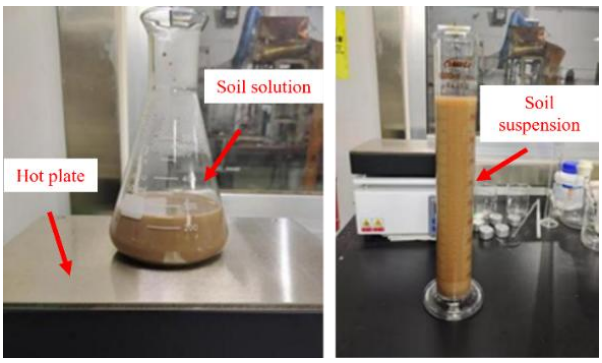

Fig. 1 - Determination process of Soil Particle Size Distribution

For the test, soil samples were passed through a 0.5 mm soil sieve. To obtain standardized soil samples, the soil was divided into three beakers and moistened with water to a pasty consistency, ensuring that each beaker received a different amount of water. After thorough mixing, the samples were left to stand for 24 hours. The liquid limit and plastic limit of the soil were determined using the fall cone method. The tests were conducted using an LP-100D liquid–plastic limit combined tester, and the procedure is illustrated in Fig. 2. The plasticity index was calculated using Equation (1)

$$I_p = W_l - W_p \quad (1)$$

where:

I_p is the plasticity index [%]; W_l is the liquid limit [%]; W_p is the plastic limit [%].

The results showed that the paddy soil samples had an average plastic limit of 15.91% and an average liquid limit of 27.99%, resulting in a plasticity index of 12.08%.

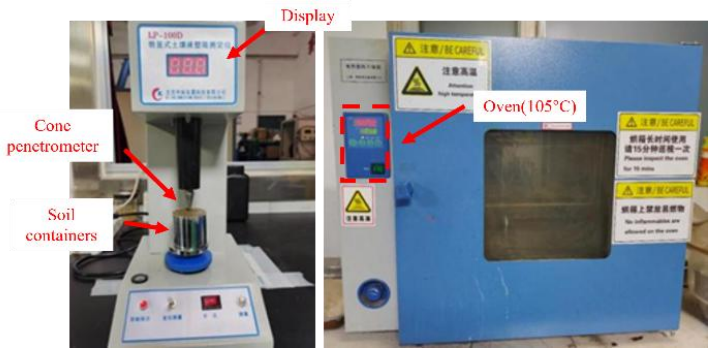

Fig. 2 - Determination process of liquid plastic limit

Sample preparation

The air-dried soil was passed through a 2-mm aperture soil sieve and subsequently oven-dried at 105°C. A predetermined mass of the dried soil was weighed, and the required moisture content for achieving target moisture levels was calculated. The calculated amount of water was uniformly mixed with the dried soil using a stirring rod. The homogenized mixture was then transferred into beakers, which were sealed with plastic film and allowed to stand for 24 hours to ensure thorough moisture equilibration. For the rotational rheometry tests, samples were prepared at four different moisture content levels: 23.0%, 26.0%, 29.0%, and 32.0%. This range was chosen to span a critical transition zone from a plastic, workable state to a near-saturated, fluid-like state, which is representative of typical field conditions encountered in paddy soils from post-tillage to pre-submergence. The increments were designed to capture potential nonlinear changes in rheological properties with increasing moisture content.

Test principles and methods

The rheological tests were conducted using a Malvern Kinexus rotational rheometer (UK). The specific parameters for the three types of tests are listed in Table 2. A parallel-plate geometry with a 25 mm plate diameter was used, and the plate gap was set to 1 mm. After setting the parameters, the sample was gently placed on the lower parallel plate, ensuring alignment with the rotor. Tests were then performed on paddy soil samples at four different moisture content levels. Data acquisition was automatically carried out by the intelligent control software integrated with the rheometer. A schematic diagram of the parallel plate configuration of the rotational rheometer is shown in Figure 3.

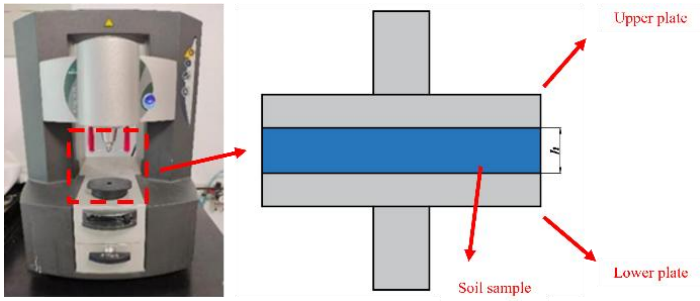

Fig. 3 - Schematic diagram of the rotational rheometer

Table 2

Parameters for steady-state and dynamic rheological tests

Test type	Parameters	Values
Steady shear test	Plate Gap/mm	1
	Shear Rate/s^{-1}	0.1～100
	Temperature/℃	25
	Number of Data Points	30
Amplitude sweep test	Plate Gap/mm	1
	Shear Strain/%	0.01~100
	Temperature/℃	25
	Frequency/Hz	1
	Number of Data Points	41
Frequency sweep test	Plate Gap/mm	1
	Frequency/Hz	0.1～100
	Temperature/℃	25
	Number of Data Points	41

The testing comprised steady-state shear tests and dynamic shear tests. The steady-state shear tests primarily measure the viscosity response of the material under varying shear rates. Viscosity, defined as the ratio of shear stress to shear rate, is used to characterize the flow properties of the material, determining whether it exhibits Newtonian behavior, shear thinning, or shear thickening *(Ma et al., 2014)*. The dynamic shear tests primarily measure the viscoelastic response of the material, distinguishing between elastic and viscous behaviors, and reflecting the structural stability of the material under external stress *(Chen et al., 2025)*. Conducting these two types of tests on paddy soil allows for a comprehensive characterization of its rheological properties *(Polanía et al., 2023)*.

The storage modulus and loss modulus are two key parameters describing a material's response under cyclic stress *(Yang et al., 2022)*. The storage modulus (G') represents the recoverable elastic strain energy stored during deformation, reflecting the material's ability to resist deformation. The loss modulus (G'') represents the energy dissipated due to internal molecular friction and structural reorganization during deformation, reflecting the viscous characteristics of the material *(Minh 2023)*. The loss factor $tan\,\delta$, defined as the ratio of the loss modulus to the storage modulus, indicates the magnitude of energy dissipation, calculated as follows:

$$tan\,\delta = \frac{G''}{G'} \tag{2}$$

For an ideal elastic body, the relationship between shear stress and strain is linear, expressed as $\tau = G\gamma$, with *G* representing the shear modulus. When analyzing oscillatory responses, the complex shear modulus G^* is commonly used in place of G. The relationship between the complex modulus and the storage modulus (G') and loss modulus (G'') is given by:

$$G^* = (G')^2 + (iG^{"})^2 \tag{3}$$

RESULTS

Steady-state shear characteristics

Apparent viscosity is a measure of fluid viscosity, characterizing the cohesive and internal frictional forces generated between molecules during flow.

It serves as a key parameter for distinguishing Newtonian from non-Newtonian fluids and reflects the ability of the internal structure of paddy soil samples to resist deformation and impede flow *(Zhang et al., 2022)* Shear rates ranging from 0.1 to 100 s^{-1} were applied to paddy soil samples with different moisture contents, and the relationship between shear rate and apparent viscosity was obtained, as shown in Figure 4.

The apparent viscosity at different moisture content is similar to the shape of the shear rate curve. At low shear rate, the apparent viscosity will decrease sharply. With the further increase of shear rate, the apparent viscosity decreases linearly. Therefore, it can be seen that paddy soil has strong non-Newtonian characteristics. The apparent viscosity decreases with the increase of shear rate, so the paddy soil has the characteristics of shear thinning. This shear-thinning behavior, typical for many concentrated suspensions and soils, is attributed to the progressive breakdown of the internal structure and alignment of particles with the flow direction.

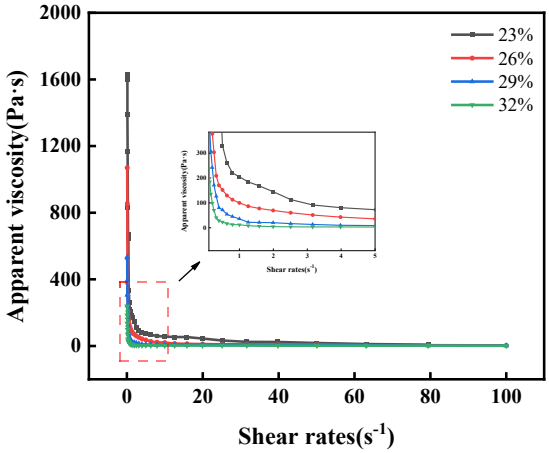

Fig. 4 - The relationship between shear rate and apparent viscosity

The fitting of apparent viscosity is shown in Figure 5. The relationship between shear rate and apparent viscosity was fitted using a power-law model; n < 1 indicates shear-thinning behavior. The apparent viscosity (η) is described by the power-law model as follows:

$$\eta = K \cdot \gamma^{n} \tag{4}$$

where: η is the apparent viscosity; K is the consistency coefficient; γ is the shear rate; n is the flow behavior index.

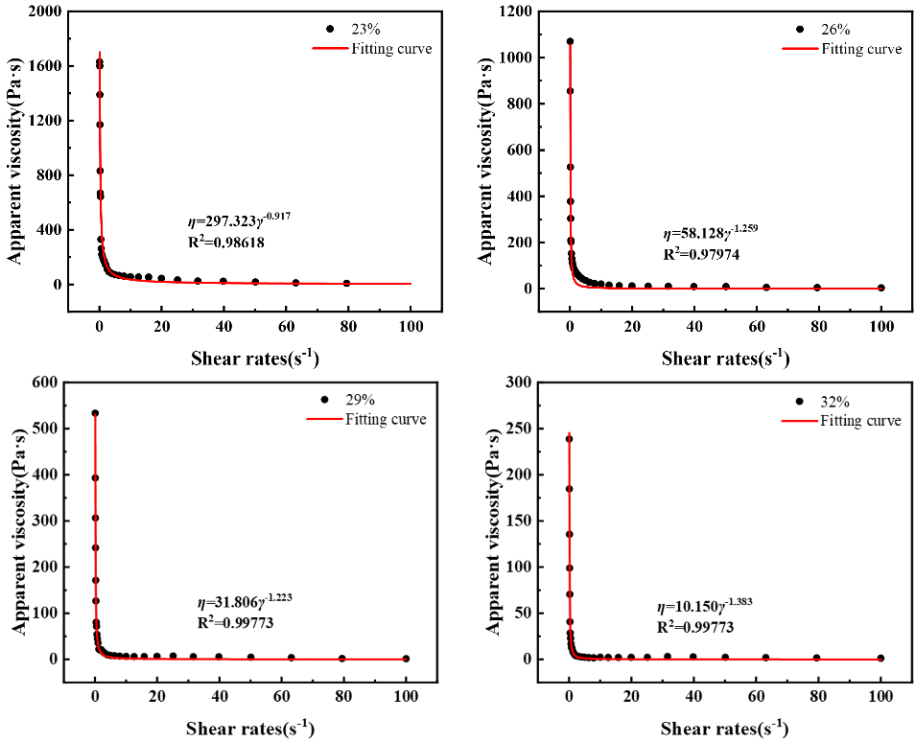

Fig. 5 - Fitting curve of apparent viscosity

The experimental results show that within the shear rate range of 0.1 to 100 s^{-1}, the viscosity of the 23% moisture content sample ranges from 11.57 to 1600 Pa·s, while that of the 32% moisture content sample ranges from 1.343 to 238.7 Pa·s. The influence of moisture content on viscosity is significant, with higher moisture content resulting in lower apparent viscosity at the same shear rate. Across the entire shear rate range, the apparent viscosity varies between 1.343 and 1600 Pa·s. The relationship between consistency coefficient and flow behavior index and moisture content is shown in Figure 6. In the experimental range, the consistency coefficient and the flow index decreased with the increase of moisture content, showing a significant negative correlation.

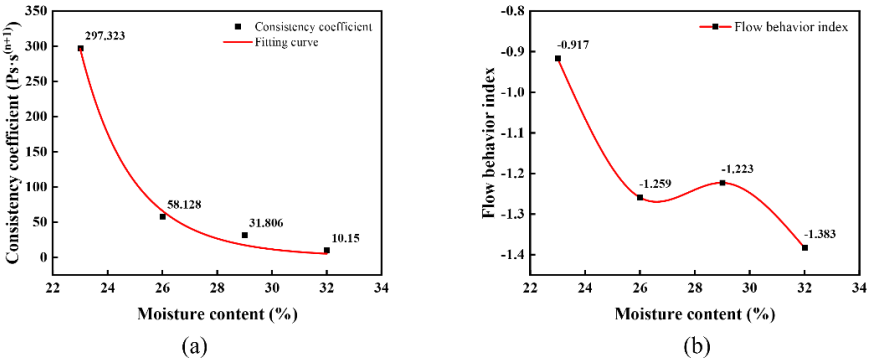

Fig. 6 - The relationship between consistency coefficient and flow behavior index

(a) The relationship between consistency coefficient and moisture content

(b) The relationship between flow behavior index and moisture content

Viscoelastic characteristics

Shear strain ranging from 0.01 to 100 was applied to paddy soil samples with different moisture contents. The relationship between shear strain and the storage modulus/loss modulus under different moisture contents is shown in Figure 7.

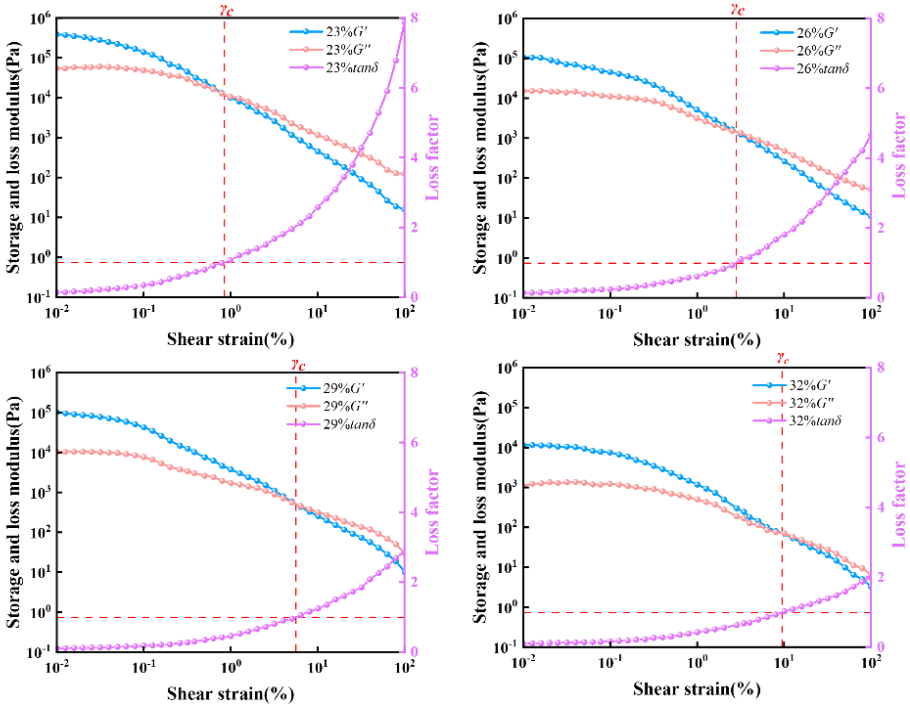

Fig. 7 - The relationship curve between shear strain and modulus

As observed in Figure 7, with increasing shear strain, both the storage modulus and loss modulus of the four sample groups decrease significantly. Under the experimental conditions, all four samples exhibit a crossover point as shear strain increases, indicating that beyond a certain shear strain, the samples undergo a transition from solid-like to liquid-like states—specifically, a shift from elastic-dominated to viscous-dominated behavior. This transition point is defined as the "flow yield strain point γ_c". Similar yield transitions have been reported in other rheological studies on soils and high-concentration slurries, marking the point where the material's internal structure is irreversibly disrupted.

In the initial stage ($\gamma < \gamma_c$), $G' > G''$, indicating the soil is in a structured state. Under minimal strain, the soil skeleton is maintained by aggregates, organic cementing agents, and meniscus water films, with stable effective stress chains existing between particles. Elastic energy storage dominates, with G' being 1-2 orders of magnitude higher than G'', exhibiting solid-like behavior. As strain increases, cementation points fracture, aggregates rotate and slide, the number of effective stress chains decreases, and the skeleton stiffness rapidly attenuates, manifested as a faster decline in G'. Simultaneously, particle sliding and water film shear generate additional dissipation, leading to a decrease in G''. When $\gamma > \gamma_c$, $G'' > G'$, and the soil transitions into a "fluid-like" state. At this point, the structural network has collapsed, and external forces are primarily dissipated through particle collisions and viscous shear of pore water, with minimal elastic energy storage. $tan\,\delta > 1$ and continues to increase, demonstrating a flow state. Higher moisture content leads to a faster attainment of a loss factor value of 1, indicating that samples with higher moisture content reach the yield point earliest—i.e., they transition from elastic to viscous dominance first, resulting in the earliest structural failure.

Figure 8 shows the variation curves of storage modulus (G') and loss modulus (G'') with shear strain for samples with different moisture contents, obtained from amplitude sweep tests. It is evident that the shapes of the variation curves are similar across different moisture contents. As moisture content increases, both storage modulus (G') and loss modulus (G'') decrease, while the loss factor increases. The data indicate that the storage modulus ranges between 10^4 and 10^6 Pa, the loss modulus between 10^3 and 10^5 Pa, and the loss factor between 0 and 8. When the shear strain is less than 0.1 %, the soil is in the linear viscoelastic region, and the loss factor does not change much, indicating that the shear effect has no obvious effect on the storage modulus and loss modulus when the shear strain is small. When the shear strain is greater than 0.1 %, the soil is outside the linear viscoelastic zone, and the loss factor increases gradually, and the increasing trend increases with the increase of shear strain, indicating that at this stage, the energy loss of the soil due to deformation is greatly increased.

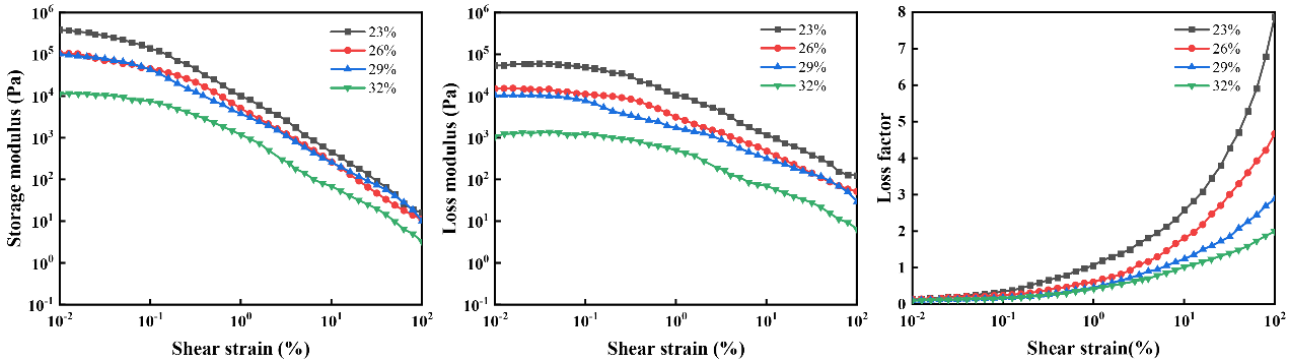

Fig. 8 - Shear parameter relationship under different moisture contents

The fitting of loss factor for different moisture contents is shown in Figure 9. It is observed that the loss factor increases in a power-law manner with shear strain, and the parameters are shown in Table 3. Analysis of the exponents of the fitted curves reveals that as moisture content increases, the exponent in the fitting equation gradually decreases (from 0.449 to 0.336), indicating that the rate of increase in loss factor with shear strain diminishes at higher moisture contents, resulting in lower energy dissipation. In high- moisture -content samples, pore water bears part of the shear stress, and energy is primarily dissipated through viscous flow of the water phase. Since water dissipation is more reversible than solid friction, the loss factor is lower compared to low-water-content samples with higher friction. A steeper slope suggests that once γ_c is exceeded, the soil rapidly loses stability, making machinery prone to "shear softening" failure.

$$tan\,\delta = a \cdot \gamma^b \tag{5}$$

where: $tan\,\delta$ is the loss factor; γ is the shear strain.

Table 3

Loss factor fitting data table under different moisture contents

Moisture content /%	Coefficient a	Index b	R^2
23	0.935	0.449	0.996
26	0.667	0.426	0.999
29	0.496	0.386	0.999
32	0.436	0.336	0.996

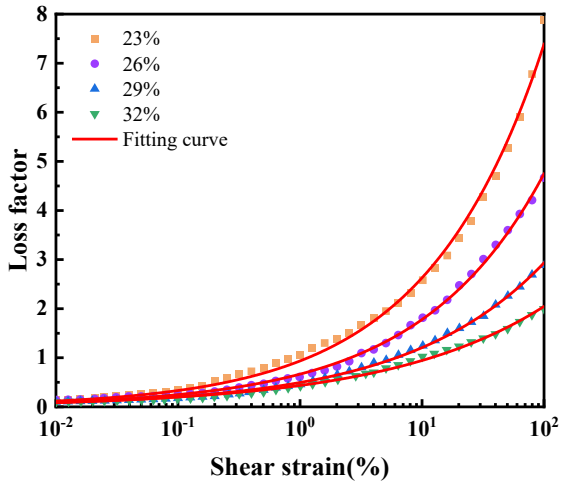

Fig. 9 - Fitting curve of loss factor under different moisture contents

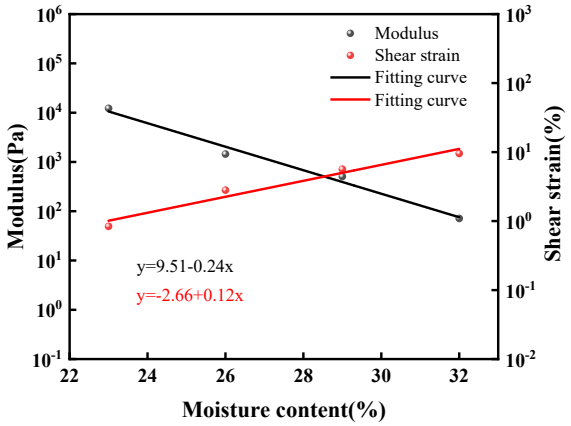

Fig. 10 - Soil yield relationship under different moisture contents

The relationship between moisture content and shear strain/modulus at the yield point is shown in Figure 10. As moisture content increases, the shear strain at the yield point increases linearly, while the modulus at the yield point decreases linearly. This clearly demonstrates that higher moisture content slows the solid-to-liquid transition and continuously reduces the structural strength of paddy soil. The increase in moisture content reduces cohesion between particles, decreases the internal friction angle, and diminishes interparticle sliding friction, collectively leading to reduced soil strength and weakened structural stability.

Frequency sweep analysis

The viscoelastic behavior of paddy soil was further characterized through frequency sweep tests conducted over a frequency range of 0.1 to 100 Hz. The results are presented in Figure 11.

In the low-frequency region (below 40 Hz), both storage modulus (G') and loss modulus (G'') exhibit minimal frequency dependence, representing a low-frequency plateau stage. Within this range, pore water has sufficient time to redistribute through soil pores, allowing external stresses to be primarily borne by pore water pressure with minimal change in effective stress between soil particles *(Campos et al., 2021)*. The soil demonstrates steady viscoelastic behavior with nearly constant G' and G'', while G'' remains slightly higher than G', corresponding to the soft-plastic state commonly observed in the tillage layer.

As frequency increases further, pore water cannot drain rapidly enough, leading to a sharp increase in effective stress. This results in a rapid rise in G', accompanied by a more moderate increase in G''. When G' exceeds G'', elastic energy storage becomes dominant over viscous dissipation, indicating a transition toward solid-like behavior of the soil structure. In this study, the crossover frequency (f^*≈40 Hz) observed in oscillatory tests marks the transition where the storage modulus becomes comparable to, or exceeds, the loss modulus under the rheometry conditions. This characteristic frequency provides an experimental reference for interpreting the dynamic stability of paddy soil subjected to high-frequency cyclic shearing; however, the excitation frequencies experienced in field operations depend on the implement, speed, boundary conditions, and loading mode.

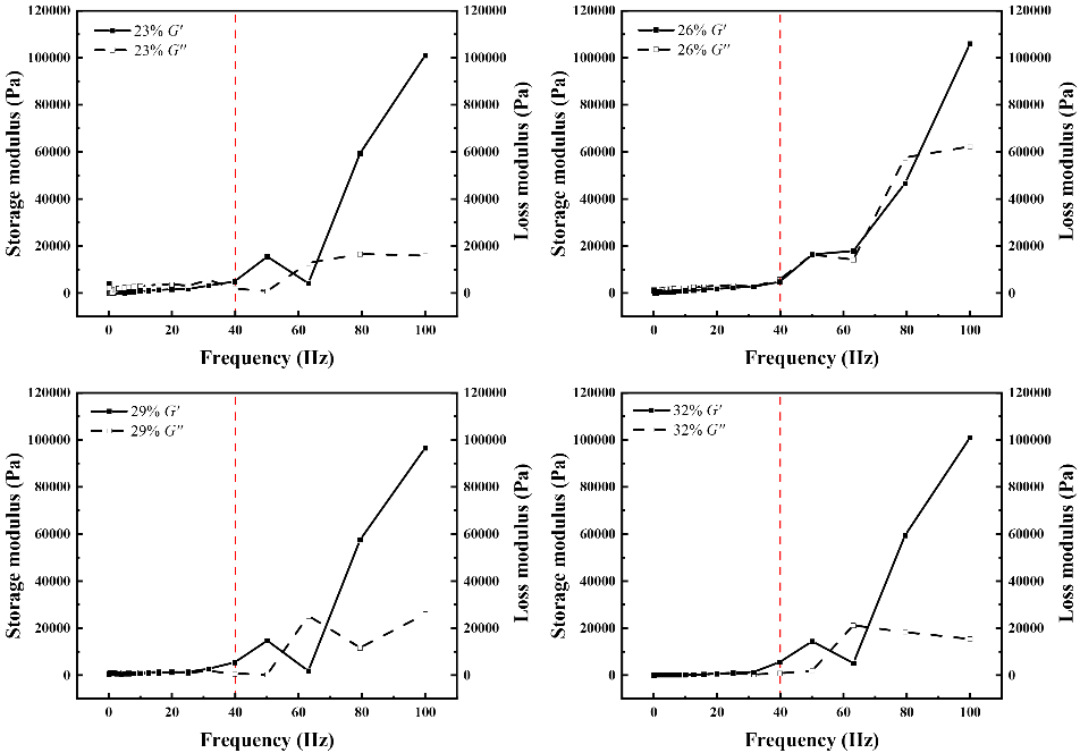

Fig. 11 - The relationship curve between frequency and modulus

The frequency dependence of the complex shear modulus can reveal the dynamic response mechanism of the viscoelastic behavior of soil. The relationship between frequency and the complex shear modulus under different moisture contents is shown in Figure 12. It can be intuitively observed that in the low-frequency region (below 40 Hz), the complex shear modulus is minimally affected by frequency. As frequency increases further, the complex shear modulus begins to increase significantly with rising frequency.

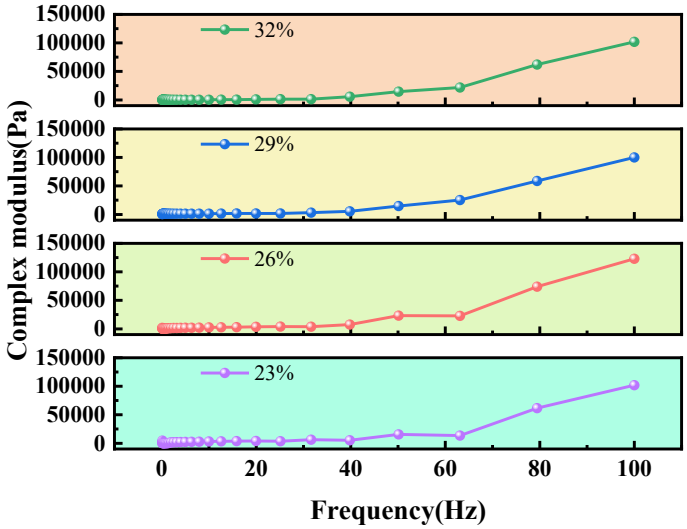

Fig. 12 - The relationship curve between frequency and complex modulus

The underlying reason for this behavior may be attributed to the fact that in the low-frequency region, soil microstructural elements—such as clay particle stacking, organic cementation, and pore water films—have sufficient time to relax or reorganize under cyclic loading. Energy is dissipated through viscous flow, and the modulus is primarily governed by long-term relaxation mechanisms. In the high-frequency region, the loading period is shorter than the soil's relaxation time, preventing timely structural adjustments and thereby enhancing the elastic response. This leads to a sharp increase in the modulus. Consequently, a critical frequency f^* can be identified as a criterion for evaluating the dynamic stability of soil. The relationship between frequency and complex viscosity under different moisture contents is illustrated in Figure 13.

It can be seen that paddy soil still exhibits shear-thinning behavior under frequency sweep conditions. This further confirms that the non-Newtonian characteristics of paddy soil are predominantly determined by microstructural breakdown mechanisms, rather than the type of loading applied.

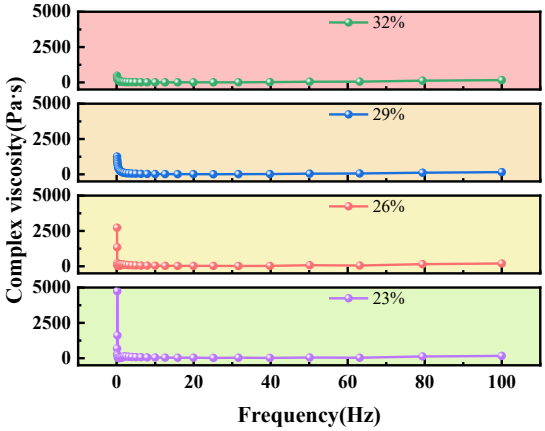

Fig. 13 - The relationship curve between frequency and complex viscosity

CONCLUSIONS

Compared with previous studies, the novelty of this work lies in revealing the rheological behavior of paddy soil under dynamic loading conditions representative of agricultural machinery operations, through a combined approach of steady-state and dynamic rheological testing. A quantitative relationship between moisture content and rheological parameters was established, providing a basis for optimizing mechanical operating parameters. In addition, the critical conditions for soil structural instability were identified, offering theoretical support for the development of anti-slip and anti-sinkage technologies in agricultural machinery. The main conclusions are as follows:

1) When the soil moisture content ranged from 23% to 32%, oscillatory tests identified a crossover frequency of approximately 40 Hz under the test conditions, indicating a transition toward elastic-dominated behavior at higher frequencies. This provides a reference for evaluating soil response under high-frequency cyclic loading.

2) As the moisture content increased from 23% to 32%, the yield modulus decreased to the order of 10^2 Pa, indicating a significant reduction in soil structural strength. Accordingly, increasing the ground contact area of agricultural machinery is necessary to mitigate the risk of sinkage.

3) The rheological results suggest that tool and running gear designs promoting gradual shearing and stable soil contact (e.g., geometries that minimize abrupt loading) can reduce tillage resistance and improve trafficability. However, further validation under soil-bin or field conditions is recommended.

REFERENCES

[1] Adebiyi A. A., & Hu P. (2021). A numerical study on impacts of sediment erosion/deposition on debris flow propagation. *Water*, 13(12): 1698. DOI: 10.3390/w13121698.

[2] Campos R., & Maciel G. (2021). Test protocol and rheological model influence on determining the rheological properties of cement pastes. *Journal of Building Engineering*, 44: 103206. DOI: 10.1016/j.jobe.2021.103206

[3] Chen Z., Fang Y., & Bezuijen A. (2025). Influence of Moisture content on Shear Strength and Tangential Adhesion Strength of Sand by a Modified Vane Shear Test Device. *International Journal of Geomechanics*, 25(2): 04024341. DOI: 10.1061/IJGNAI.GMENG-10366.

[4] Hu Z. (2024). *Research on soft ground trafficability of tracked vehicle based on soil dynamic bearing model.* (Master). Shandong Jiaotong University, Retrieved from https://link.cnki.net/doi/10.27864/d.cnki.gsjtd.2024.000021 Available from Cnki

[5] JI C., & Zhao C. (2004). Development of a dynamic load paddy soil rheometer. Transactions of the Chinese Society for Agricultural Machinery (02): 88–91.

[6] Khramchenkov M. (2003). Mathematical modeling of rheological properties of clays and clay rocks. *Journal of engineering physics and thermophysics*, 76(3): 659–666. DOI: 10.1023/A:1024745719897.

[7] Liang X., Shi Y., Qin Y., Yao Y., Zhang H., & Wang Y. (2024). Experiment on rheological properties of

tidal flat soil under different moisture content and standing time. *Transactions of the Chinese Society of Agricultural Engineering*, 40(01): 182–190. DOI: 10.11975/j.issn.1002-6819.202309143.

[8] Liang Z., Zhang A., Ren W., Hu N., Wang Y., & Li S. (2023). Rheological properties of Yili loess with different moisture content and high soluble salt content. *Transactions of the Chinese Society of Agricultural Engineering*, 39(05): 90–99. DOI: 10.11975/j.issn.1002-6819.202211035

[9] Luo D., Zhu G., & Jiang C. (1990). Study on Rheological Theory of Paddy Soil and Its Application. Journal of Wuhan University of Technology(Information & Management Engineering)(02): 1–9.

[10] Ma W.-b., Rao Q.-h., Li P., Guo S.-c., & Feng K. (2014). Shear creep parameters of simulative soil for deep-sea sediment. *Journal of Central South University*, 21(12): 4682–4689. DOI: 10.1007/s11771-014-2477-3.

[11] Minh N. N. (2023). Rheological properties of yam mucilage. *Korea-Australia Rheology Journal*, 35(4): 323–333. DOI: 10.1007/s13367-023-00071-0.

[12] Ministry of Water Resources of the People's Republic of China. (2019). Standard for geotechnical testing method (GB/T 50123-2019). Beijing: China Planning Press.

[13] Nachtergaele F., & Spaargaren O. International Society of Soil Science. ISRIC. FAO. Acco. Leuven.

[14] Ni H., & Huang Y. (2020). Rheological study on influence of mineral composition on viscoelastic properties of clay. *Applied Clay Science*, 187: 105493. DOI: 10.1016/j.clay.2020.105493.

[15] Pan J. (1983). Soil characteristics of paddy field in southern China and reasonable structure of paddy field walking device. Tractor & Farm Transporter (02): 6–11.

[16] Polanía O., Cabrera M., Renouf M., Azéma E., & Estrada N. (2023). Grain size distribution does not affect the residual shear strength of granular materials: An experimental proof. *Physical Review E*, 107(5): L052901. DOI: 10.1103/physreve.107.l052901

[17] Rakshith S., Zhang X., Coussot P., & Singh D. (2018). Complex-Fluid Approach for Determining Rheological Characteristics of Fine-Grained Soils and Clay Minerals. *Journal of Materials in Civil Engineering*, 30(12): 04018322. DOI: 10.1061/(asce)mt.1943-5533.0002543.

[18] Sun L., Pan Y., Wang Y., Xiao K., Wang J., Zhao Y., & Liao Y. (2022). The Effects of Multiple Parameters on Initial Apparent Viscosity and Rheological Behavior in a Liquid-Phase Paddy Field. *Journal of the ASABE*, 65(5): 1141–1148. https://doi.org/10.13031/ja.15178

[19] Tian X. (2023). *Study on nonlinear creep characteristics and long-term strength of expansive soil improved by microorganism.* (Master). Central South University of Forestry and Technology, Retrieved from https://link.cnki.net/doi/10.27662/d.cnki.gznlc.2023.000144 Available from Cnki

[20] USDA N. (1999). United States department of agriculture. Natural Resources Conservation Service. Plants Database. http://plants. usda. gov (accessed in 2000).

[21] Wei W., Jiafeng Z., Chenhui S., & Xiaoliang Z. (2017). Design and Experiment of Integrated Test System for Terramechanics Parameters. *Transactions of the Chinese Society of Agricultural Machinery*, 48(5). DOI: 10.6041/j.issn.1000-1298.2017.05.008.

[22] Xu G.-Z., Gao Y.-F., Zhang Y., & Sun R.-B. (2017). Rheological behavior of dredged slurries at high moisture contents. *Marine Georesources & Geotechnology*, 35(3): 357–364. DOI: 10.1080/1064119x.2016.1173747.

[23] Yang C., Wang J., Xie J., Wu S., Amirkhanian S., Wang F., Zhang L., & Hu J. (2022). Investigation on rheological properties of bitumen based on rheological parameters of maltenes. *Road Materials and Pavement Design*, 23(4): 942–957. DOI: 10.1080/14680629.2020.1860805.

[24] Zhang S., Song T., Hao X., Zhang L., & Chen J. (2023). Study on rheological properties of red mud and applicability of rheological model. *Journal of China Three Gorges University (Natural Sciences)*, 45(01): 48–53. 10.13393/j.cnki.issn.1672-948x.2023.01.008.

[25] Zhang Z.-L., Cui Z.-D., & Zhao L.-Z. (2022). Modeling shear behavior of sand-clay interfaces through two-dimensional distinct element method analysis. *Environmental Earth Sciences*, 81(5): 140. DOI: 10.1007/s12665-022-10244-9.